

described by Sternglanz et al.²¹ occurring in barium adenosine 5'-phosphate heptahydrate where a completely hydrated barium ion is attached to the adenosine 5'-phosphate moiety *only* through hydrogen bonds from coordinated water molecules is not analogous to the above situations. In fact, such indirect metal-water-anion interactions, where there is not other direct ligand metal binding, are not uncommon and occur usually whenever the anion contains suitable hydrogen bonding sites. For example, in $[\text{Mg}(\text{H}_2\text{O})_6]\text{H}_2\text{EDTA}^{12}$ and $[\text{Mg}(\text{H}_2\text{O})_6]\text{Cr}_2\text{O}_7 \cdot 2(\text{CH}_2)_6\text{N}_4^{13}$ the $\text{Mg}(\text{H}_2\text{O})_6^{2+}$ ion is hydrogen bonded to dihydrogen ethylenediaminetetraacetate and hexamethylenetetramine, respectively, although no direct Mg(II) interactions with H_2EDTA or $(\text{CH}_2)_6\text{N}_4$ exist.

- (21) Sternglanz, H.; Subramanian, E.; Lacy, J. C., Jr.; Bugg, C. E. *Biochemistry* **1976**, *15*, 4797.
- (22) Furberg, S.; Mostad, A. *Acta Chem. Scand.* **1962**, *16*, 1627.
- (23) Shefter, E.; Trueblood, K. N. *Acta Crystallogr.* **1965**, *18*, 1067.
- (24) DeMeester, P.; Goodgame, D. M. L.; Skapski, A. C.; Smith, B. T. *Biochim. Biophys. Acta* **1974**, *340*, 113.
- (25) Collins, A. D.; DeMeester, P.; Goodgame, D. M. L.; Skapski, A. C. *Biochim. Biophys. Acta* **1975**, *402*, 1.
- (26) Gunstone, F. C. "Basic Stereochemistry"; The English Universities Press Ltd.: London, 1974; pp 49-58.
- (27) Siegel, H.; Fischer, B. E.; Priejs, B. *J. Am. Chem. Soc.* **1977**, *99*, 4489.

Contribution from the Department of Chemistry,
University of California, Berkeley, California 94720

Coordination Chemistry of Microbial Iron Transport Compounds. 17.¹ Preparation and Structural Characterization of Tris(*N*-methylthiobenzohydroxamato)cobalt(III), -chromium(III), -iron(III), and -manganese(III)

DEREK P. FREYBERG, KAMAL ABU-DARI,² and KENNETH N. RAYMOND*

Received May 8, 1979

The preparation and isolation of tris(*N*-methylthiobenzohydroxamato)cobalt(III), -chromium(III), -iron(III), and -manganese(III) are reported. The structures of these four compounds have been determined by single-crystal X-ray diffraction using automated-counter methods. The complexes are isostructural in the cis configuration, with the metal environment being a trigonally distorted octahedron, though the manganese complex displays considerable tetragonal distortion. The twist angle (the projection of the top trigonal face on the bottom one) averages 54.9° for the Co complex, 48.7° for the Cr, 42.9° for the Fe, and 46.0° for the Mn; these are 60° and 0° for octahedral and trigonal-prismatic structures, respectively. The M-S bond lengths average 2.203 (3) Å for Co, 2.367 (8) Å for Cr, and 2.445 (14) Å for Fe, while the M-O bond lengths average 1.935 (5), 1.976 (6), and 1.990 (5) Å, respectively. The axial (tetragonal axis) and equatorial bond lengths for the Mn-S bonds are 2.584 (1) and 2.339 (15) Å and for Mn-O are 2.132 (2) and 1.950 (9) Å, respectively. The average S-M-O chelate angles are 87.3 (3), 82.6 (1), 80.1 (2), and 80.6 (11)° for M = Co, Cr, Fe, and Mn. The changes in M-S bond lengths and trigonal twist angles of the complexes are ascribed to ligand field effects. The structure of Cr(MTB)₃ (MTB = *N*-methylthiobenzohydroxamate anion) was solved by direct phasing methods followed by full-matrix least-squares and Fourier techniques, while the other structures were refined by using atomic coordinates from the Cr complex. Green crystals of Co(MTB)₃ conform to the space group $P2_1/n$ with $a = 11.805$ (2), $b = 12.182$ (2), $c = 18.230$ (4) Å, and $\beta = 92.12$ (2)°; $V = 2620$ (2) Å³; $Z = 4$; $\rho_{\text{calcd}} = 1.41$ and $\rho_{\text{obsd}} = 1.41$ (1) g cm⁻³. Refinement using the 3862 reflections with $F^2 > 3\sigma(F^2)$, with all nonhydrogen atoms given anisotropic temperature factors, gave $R = 3.4\%$ and $R_w = 4.2\%$. Green crystals of Cr(MTB)₃ have $a = 11.698$ (4), $b = 12.080$ (3), $c = 18.851$ (6) Å, and $\beta = 93.81$ (3)°; $V = 2658$ (3) Å³; $\rho_{\text{calcd}} = 1.38$ and $\rho_{\text{obsd}} = 1.36$ (1) g cm⁻³. The 3207 reflections with $F^2 > 3\sigma(F^2)$ gave $R = 3.2$ and $R_w = 4.2\%$. Violet crystals of Fe(MTB)₃ have $a = 11.668$ (2), $b = 12.037$ (2), $c = 19.013$ (4) Å, and $\beta = 94.94$ (2)°; $V = 2661$ (2) Å³; $\rho_{\text{calcd}} = 1.38$ and $\rho_{\text{obsd}} = 1.36$ (1) g cm⁻³. The 3070 reflections with $F^2 > 3\sigma(F^2)$ gave $R = 3.3\%$ and $R_w = 3.8\%$. Green crystals of Mn(MTB)₃ have $a = 11.604$ (3), $b = 12.044$ (3), $c = 18.990$ (6) Å, and $\beta = 94.87$ (2)°; $V = 2644$ (3) Å³; $\rho_{\text{calcd}} = 1.39$ and $\rho_{\text{obsd}} = 1.38$ (1) g cm⁻³. The 3452 reflections with $F^2 > 3\sigma(F^2)$ gave $R = 3.5\%$ and $R_w = 3.8\%$.

Introduction

The siderophores are low-molecular-weight compounds which are manufactured by microbes in order to facilitate the uptake of ferric iron.^{3,4} The insolubility of ferric hydroxide at physiological pH [$(\text{Fe}^{3+}) \approx 10^{-18}$ M at pH 7 on the basis of $K_{\text{sp}} \approx 10^{-39}$]⁵ and the essential nature of iron for microbial growth apparently engendered the production of a wide range of powerful sequestering agents—the siderophores. The common functional groups in these siderophores are hydroxamate, as in ferrichromes⁶ and ferrioxamines,⁷ and catecholate, as in enterobactin.⁸ A potentially new type of chelate moiety belonging to the siderophore class of compounds came with the discovery that cupric and ferric complexes of *N*-methylthioformhydroxamic acid could be isolated from culture broths of *Pseudomonas fluorescens* grown on *n*-paraffin or sucrose as the only source of carbon.^{9,10} The three siderophore chelate groups are shown in Figure 1.

We have reported the preparation and resolution of the thiobenzohydroxamate complexes of Cr(III), Fe(III), and Co(III),¹¹ where we predicted the compounds to have a cis geometry on the basis of their circular dichroism spectra and physical properties. Subsequently, Murray et al. have reported electrochemical and magnetic studies of tris(thiobenzohydroxamato)iron(III)¹² and the crystal structure of tris(*N*-methylthioformhydroxamato)iron(III),¹³ which was found

to have the cis geometry. Leong and Bell¹⁴ have reported the synthesis and separation of the geometrical isomers of *N*-methylthioformhydroxamate complexes of Cr(III), Rh(III), and Pt(II). In a contradiction of Murray's report,¹² we have found that tris(thiobenzohydroxamato)iron(III) is high spin from 5 K to room temperature and, under suitable conditions, undergoes reversible electrochemical reduction.¹⁵

High-spin ferric iron and manganic ion are identical in ionic radius, while chromic and low-spin cobaltic ions are somewhat smaller.¹⁶ The geometries of the metal(III) complexes are of interest both to characterize the coordination sites of the siderophore complexes and to determine the fundamentals of the coordination chemistry of the thiohydroxamate-transition-metal complexes, including the degree to which other complexes mimic the naturally occurring ferric siderophores. The influence of the d-electron configuration on the coordination geometry within this isostructural series is a strong secondary interest. We report here the preparation and single-crystal structural analyses of tris(*N*-methylthiobenzohydroxamato)cobalt(III), -chromium(III), -iron(III), and -manganese(III).

Experimental Section

Sodium *N*-methylthiobenzohydroxamate was prepared by a method analogous to that used to prepare the *N*-unsubstituted acid salt.¹⁷ The tetrahydrofuran adduct of chromic chloride, $\text{CrCl}_3 \cdot 3\text{THF}$, was

Table I. Summary of Crystal Data for $M(\text{PhC}(=\text{S})\text{N}(\text{O})\text{CH}_3)_3^a$

	M = Co	M = Cr	M = Fe	M = Mn
mol wt	557.60	550.67	554.52	553.61
cell const ^b				
<i>a</i> , Å	11.805 (2)	11.698 (4)	11.668 (2)	11.604 (3)
<i>b</i> , Å	12.182 (2)	12.080 (3)	12.037 (2)	12.044 (3)
<i>c</i> , Å	18.230 (4)	18.851 (6)	19.013 (4)	18.990 (6)
β, deg	92.12 (2)	93.81 (3)	94.94 (2)	94.87 (2)
cell vol, Å ³	2620 (2)	2658 (3)	2661 (2)	2644 (3)
<i>d</i> _{calcd} , g cm ⁻³	1.41	1.38	1.38	1.39
<i>d</i> _{obsd} , g cm ⁻³	1.41 (1)	1.36 (1)	1.36 (1)	1.38 (1)
cryst dimens, mm	0.20 × 0.35 × 0.50	0.15 × 0.35 × 0.60	0.15 × 0.30 × 0.35	0.15 × 0.30 × 0.30
abs coeff μ, cm ⁻¹	9.1	6.7	8.2	7.4

^a For all compounds: space group $P2_1/n$; $Z = 4$ formula units/cell. ^b Ambient temperature of 23 °C; Mo $K\alpha_1$ radiation (λ 0.709 30 Å).

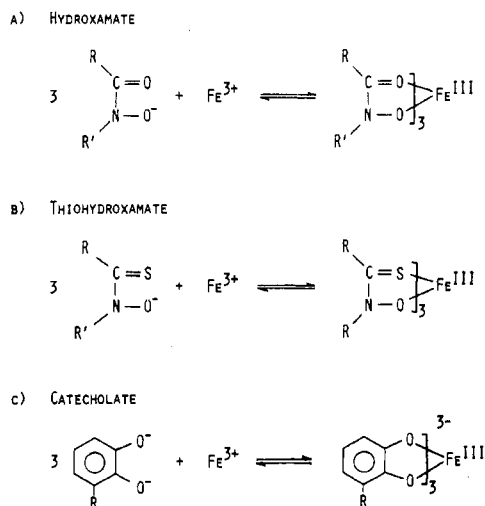


Figure 1. Reaction with ferric ion of the three siderophore chelating groups: (A) hydroxamate; (B) thiohydroxamate; (C) catecholate.

prepared by a literature method¹⁸ and protected from moisture.

Co-, Cr-, Fe-, and Mn(MTB)₃ (MTB = *N*-methylthiohydroxamate anion) were prepared by methods analogous to those used for the *N*-unsubstituted complexes.^{11,19-21} The materials were recrystallized from chloroform/ethanol solution by slow evaporation. Crystals suitable for data collection were mounted in glass capillaries. Densities were determined by flotation in iodoethane/heptane mixtures.

Unit Cell and Diffraction Data

For each crystal, preliminary cell dimensions were obtained by using the program SEARCH²² to obtain the positions of 25 reflections. Laue symmetry of $2/m$ was observed for each complex, with $h0l$, $h+l = 2n$, and $0k0$, $k = 2n$, defining the space group as $P2_1/n$ (an alternate setting of $P2_1/c$, No. 14). Crystal data, obtained by a least-squares fit to the setting angles of 22 accurately centered, high-angle reflections, are given in Table I.

Intensity data were collected on an Enraf-Nonius CAD-4 automated diffractometer controlled by a PDP-8/E computer and using monochromatic Mo $K\alpha$ radiation. The intensities of a unique set of reflections ($+h, +k, \pm l$) with $2^\circ < 2\theta < 50^\circ$ were measured by using the θ - 2θ scan technique. The duplicates $0, k, -l$ were also measured for Co-, Fe-, and Mn(MTB)₃, as a check. The θ scan angle was calculated as $(0.60 + 0.347 \tan \theta)^\circ$ for Co, Fe, and Mn and $(0.70 + 0.347 \tan \theta)^\circ$ for Cr; and an aperture with a height of 4 mm and a variable width [width (mm) = $2.0 + 1.0 \tan \theta$ for Co, Fe, and Mn; $2.5 + 0.5 \tan \theta$ for Cr] was located 173 mm from the crystal. The scan time was variable, with a maximum of 80 s for Co, Cr, and Mn and 60 s for Fe. The intensities of three standard reflections were monitored regularly and showed no significant fluctuations. Three orientation standard reflections were also monitored and showed no change in setting angles greater than 0.1° in any axis. An attenuator, decreasing the intensity of the diffracted beam by a factor of 18.17, was inserted into the beam when the prescan indicated an intensity too high for accurate counting ($I > 50\,000$ counts/s).

The data (4722 for Co, 3458 for Cr, 3726 for Fe, and 4410 for Mn) were reduced to F^2 and $\sigma(F^2)$ as described previously^{22,23} and averaged, giving 4526 independent reflections for Co (R factor for

averaging 196 reflections: 1.4%), 3207 for Cr, 3545 for Fe ($R = 1.8\%$ for 181 reflections), and 4226 for Mn ($R = 1.4\%$ for 184 reflections). The parameter p , introduced to prevent overweighting of the strong reflections,²⁴ was set to 0.03 for Co, Fe, and Mn and 0.04 for Cr. Lorentz and polarization corrections were made (including a correction for the polarization of the graphite monochromator), but neither decomposition nor absorption corrections were considered necessary.

Solution and Refinement of the Structures

Chromium. The positions of the Cr and three S atoms were obtained by use of the MULTAN²⁵ program series, using 300 E values, and these led to location of all nonhydrogen atoms by standard difference Fourier and least-squares techniques.²⁵⁻²⁷ At this point, all hydrogens were visible in a difference Fourier. After anisotropic refinement of the nonhydrogen atoms, the phenyl hydrogens were introduced as fixed atoms (C-H distance 0.97 Å, bisecting the C-C-C angle) with $B = 5.0 \text{ \AA}^2$, and the methyl hydrogens were introduced as rigid groups (C-H distance 0.97 Å, bond angle 109.5°) centered on the methyl carbons, with $B = 7.0 \text{ \AA}^2$, and only the rotation angle about the nitrogen-(methyl carbon) vector was allowed to vary. Full-matrix least-squares refinement with 310 variables, using the 3207 reflections with $F^2 > 3\sigma(F^2)$, led to convergence with $R = 3.2\%$, $R_w = 4.2\%$, and E , the error in an observation of unit weight, of 1.48. A final difference Fourier was featureless.

Cobalt. The positions of the nonhydrogen atoms were obtained from the isostructural Cr complex, and solution and refinement proceeded in the same way. Full-matrix least-squares refinement with 310 variables, using the 3862 reflections with $F^2 > 3\sigma(F^2)$, led to convergence with $R = 3.4\%$, $R_w = 4.2\%$, and $E = 1.58$. A final difference Fourier was featureless.

Iron. Refinement was as for the cobalt complex, using the 3070 reflections with $F^2 > 3\sigma(F^2)$ led to convergence with $R = 3.3\%$, $R_w = 3.8\%$, and $E = 1.36$.

Manganese. Refinement was as for the cobalt complex, using the 3452 reflections with $F^2 > 3\sigma(F^2)$ led to convergence with $R = 3.5\%$, $R_w = 3.8\%$, and $E = 1.34$.

Tables II-V give the positional and anisotropic thermal parameters for the nonhydrogen atoms for Co, Cr, Fe, and Mn, respectively, while the positional and isotropic thermal parameters for the hydrogen atoms are given in Tables X-XIII.²⁸ Root-mean-square amplitudes of vibration for the nonhydrogen atoms are given in Tables XIV-XVII,²⁸ while Tables XVIII-XXI²⁸ have listings of the observed and calculated structure factors.

Description and Discussion of the Structures

A perspective view of Cr(MTB)₃ with the numbering scheme used (the same scheme is used also for the other complexes) is shown in Figure 2. Each molecule contains three five-membered rings consisting of the metal atom and a thiohydroxamate group. The rings are arranged in the cis geometry, with the metal atom in approximate octahedral coordination. The coordination is most nearly octahedral for Co (a low-spin d^6 configuration), as expected from ligand field theory, with Cr and Fe showing an increased trigonal distortion and Mn (d^4) showing a substantial tetragonal distortion. Bond lengths and angles for the complexes are given in Tables VI and VII, respectively. Figure 3 is a stereoscopic view of the molecular packing, again for Cr(MTB)₃. The molecules are neutral and well separated, with the nearest nonhydrogen

Table II. Positional and Anisotropic Thermal Parameters ($\times 10^4$) for the Nonhydrogen Atoms of Cr(MTB)₃

atom	x	y	z	β_{11}^a	β_{22}	β_{33}	β_{12}	β_{13}	β_{23}
Co	0.24409 (3)	0.15401 (3)	0.43482 (2)	38.8 (3)	43.6 (3)	18.0 (1)	-2.0 (2)	-1.9 (1)	0.4 (2)
S ₁	0.21746 (7)	0.31226 (6)	0.49067 (4)	56.3 (6)	44.3 (6)	19.7 (2)	-10.9 (5)	2.8 (3)	-1.1 (3)
S ₂	0.38855 (6)	0.21639 (7)	0.37447 (4)	46.1 (6)	60.7 (6)	18.4 (2)	0.1 (5)	0.1 (3)	7.9 (3)
S ₃	0.12470 (6)	0.19989 (7)	0.34443 (4)	47.8 (6)	50.0 (6)	22.6 (2)	11.8 (5)	-7.5 (3)	-4.7 (3)
O ₁	0.1301 (2)	0.0918 (2)	0.4963 (1)	52 (2)	48 (2)	25.7 (7)	-12 (1)	6.8 (9)	-5.2 (9)
O ₂	0.3529 (2)	0.1068 (2)	0.5095 (1)	44 (2)	54 (2)	20.4 (6)	-10 (1)	-2.7 (8)	8.3 (8)
O ₃	0.2531 (2)	0.0106 (2)	0.3887 (1)	56 (2)	50 (2)	20.6 (6)	8 (1)	-8.5 (8)	-1.9 (8)
N ₁	0.0924 (2)	0.1603 (2)	0.5481 (1)	49 (2)	54 (2)	23.4 (8)	-13 (2)	5 (1)	-1 (1)
N ₂	0.4605 (2)	0.1436 (2)	0.5022 (1)	42 (2)	37 (2)	20.7 (8)	-3 (1)	-4.6 (9)	3 (1)
N ₃	0.2051 (2)	0.0043 (2)	0.3201 (1)	47 (2)	46 (2)	20.6 (8)	2 (2)	-2 (1)	-3 (1)
C ₁₁	0.0144 (3)	0.1050 (3)	0.5972 (2)	89 (3)	85 (3)	41 (1)	-39 (3)	27 (2)	-4 (2)
C ₁₂	0.1249 (2)	0.2619 (3)	0.5528 (2)	46 (2)	53 (2)	23 (1)	-6 (2)	1 (1)	0 (1)
C ₁₃	0.0869 (3)	0.3350 (3)	0.6117 (2)	66 (3)	57 (3)	25 (1)	-14 (2)	11 (1)	-5 (1)
C ₁₄	0.0107 (3)	0.4186 (3)	0.5951 (2)	72 (3)	65 (3)	41 (1)	-4 (2)	14 (2)	-3 (2)
C ₁₅	-0.0201 (4)	0.4910 (3)	0.6502 (3)	94 (4)	68 (3)	67 (2)	-9 (3)	36 (3)	-12 (2)
C ₁₆	0.0238 (5)	0.4817 (4)	0.7184 (3)	138 (5)	109 (5)	51 (2)	-21 (4)	40 (3)	-31 (3)
C ₁₇	0.0981 (5)	0.3988 (5)	0.7362 (2)	165 (6)	151 (6)	25 (1)	-42 (5)	21 (2)	-14 (2)
C ₁₈	0.1308 (4)	0.3240 (3)	0.0825 (2)	117 (4)	91 (4)	27 (1)	-4 (3)	8 (2)	-1 (2)
C ₂₁	0.5292 (3)	0.1266 (3)	0.5699 (2)	62 (3)	60 (3)	23 (1)	-1 (2)	-12 (1)	6 (1)
C ₂₂	0.4908 (2)	0.1909 (2)	0.4420 (2)	44 (2)	35 (2)	21.1 (9)	2 (2)	0 (1)	1 (1)
C ₂₃	0.6100 (2)	0.2220 (2)	0.4289 (2)	43 (2)	43 (2)	28 (1)	-1 (2)	4 (1)	-1 (1)
C ₂₄	0.6312 (3)	0.3227 (3)	0.3965 (2)	54 (3)	50 (3)	45 (1)	5 (2)	12 (2)	10 (2)
C ₂₅	0.7415 (3)	0.3526 (3)	0.3818 (3)	72 (3)	59 (3)	75 (2)	-4 (3)	29 (2)	21 (2)
C ₂₆	0.8292 (3)	0.2828 (4)	0.3984 (3)	50 (3)	86 (4)	82 (4)	-5 (3)	26 (2)	13 (2)
C ₂₇	0.8093 (3)	0.1819 (3)	0.4292 (3)	48 (3)	74 (3)	66 (2)	14 (2)	12 (2)	12 (2)
C ₂₈	0.6993 (3)	0.1511 (3)	0.4445 (2)	51 (2)	51 (2)	43 (1)	1 (2)	3 (1)	8 (2)
C ₃₁	0.2270 (3)	-0.1014 (3)	0.2852 (2)	82 (3)	48 (2)	31 (1)	13 (2)	-3 (2)	-11 (1)
C ₃₂	0.1449 (2)	0.0848 (3)	0.2922 (2)	39 (2)	57 (2)	20.2 (9)	3 (2)	-3 (1)	-2 (1)
C ₃₃	0.0956 (3)	0.0823 (3)	0.2167 (2)	58 (2)	50 (2)	21 (1)	5 (2)	-6 (1)	-2 (1)
C ₃₄	-0.0197 (3)	0.1013 (3)	0.2044 (2)	59 (3)	69 (3)	25 (1)	-3 (2)	-9 (1)	0 (1)
C ₃₅	-0.0644 (3)	0.1067 (3)	0.1332 (2)	77 (3)	65 (3)	34 (1)	-1 (2)	-23 (2)	4 (2)
C ₃₆	0.0039 (4)	0.0936 (3)	0.0751 (2)	120 (4)	52 (3)	25 (1)	7 (3)	-20 (2)	-2 (1)
C ₃₇	0.1164 (4)	0.0749 (3)	0.0862 (2)	119 (4)	92 (4)	20 (1)	23 (3)	5 (2)	-2 (2)
C ₃₈	0.1633 (3)	0.0697 (3)	0.1571 (2)	72 (3)	95 (4)	24 (1)	22 (3)	-1 (1)	0 (2)

^a The form of the anisotropic thermal ellipsoid is $\exp[-(\beta_{11}h^2 + \beta_{22}k^2 + \beta_{33}l^2 + 2\beta_{12}hk + 2\beta_{13}hl + 2\beta_{23}kl)]$.

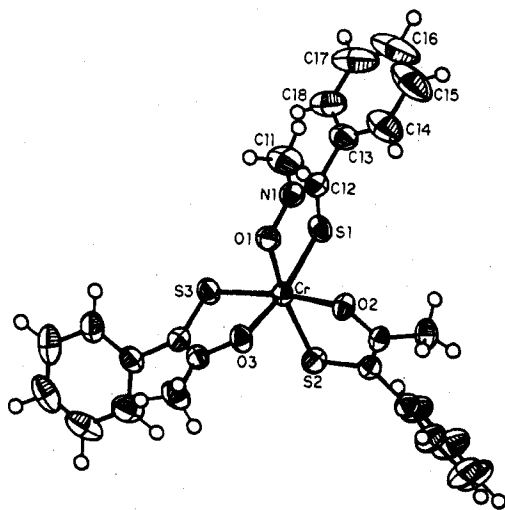


Figure 2. ORTEP drawing of Cr(MTB)₃, viewed down the approximate molecular threefold axis, with the numbering scheme of the nonhydrogen atoms. The nonhydrogen atoms are drawn at 50% probability contours of the thermal motion, while the hydrogen atoms have an arbitrary size.

intermolecular contacts being approximately 3.2 Å for each complex. Figure 4 shows the metal atom coordination polyhedron, with some of the features tabulated for each complex.

Other features of the molecular geometry of these complexes such as the dihedral angles between the chelate planes and the phenyl rings seem essentially independent of the metal coordination and are determined by packing considerations. Though the thiohydroxamate chelates are close to planar (Table VIII²⁸), the distance of the metal atom from the chelate

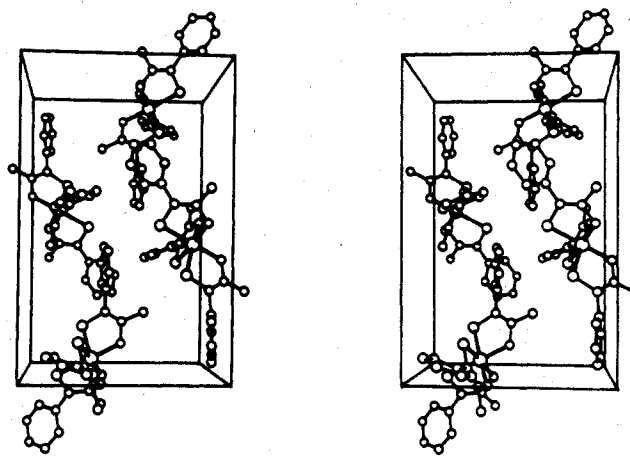


Figure 3. Stereoscopic packing diagram of Cr(MTB)₃, with the unit cell edges shown; *b* is horizontal, *c* is vertical, and *a* is into the paper.

plane varies from less than 0.2 to greater than 0.6 Å. This variation is also believed to be due to molecular packing, as the less hindered tris(*N*-methylthioformhydroxamato)iron(III) complex¹³ has crystallographic C₃ symmetry with the Fe atom 0.34 Å from the chelate plane.

We have previously reported the structures of tris(catecholato)chromate(III) and -ferrate(III)²⁹ and that of tris(benzohydroxamato)chromium(III)²³ and have examined the structural differences between the chromic and ferric complexes of these two ligands. In the present work we report the structures of four complexes with the *N*-methylthiobenzohydroxamate anion and extend a similar comparison. These MTB complexes exist, both in solution and in the solid state, in the *cis* geometry with approximately trigonal symmetry; and their isostructural nature facilitates comparisons of the

Table III. Positional and Anisotropic Thermal Parameters ($\times 10^4$) for the Nonhydrogen Atoms of Cr(MTB)₃

atom	x	y	z	β_{11}^a	β_{22}	β_{33}	β_{12}	β_{13}	β_{23}
Cr	0.23815 (4)	0.15663 (4)	0.43438 (2)	44.6 (4)	48.8 (4)	18.1 (1)	-1.2 (3)	-1.3 (2)	-0.5 (2)
S ₁	0.19828 (7)	0.32657 (7)	0.49214 (4)	69.1 (7)	50.1 (6)	20.5 (2)	-10.7 (5)	3.1 (3)	-1.7 (3)
S ₂	0.39693 (6)	0.22381 (7)	0.37652 (4)	55.4 (6)	74.0 (7)	19.3 (2)	0.4 (5)	1.4 (3)	10.3 (3)
S ₃	0.11321 (7)	0.20371 (7)	0.33564 (4)	62.0 (6)	57.5 (6)	22.9 (2)	17.1 (5)	-7.9 (3)	-6.2 (3)
O ₁	0.1252 (2)	0.0981 (2)	0.4975 (1)	59 (2)	53 (2)	26.0 (7)	-15 (1)	8.8 (8)	-7.1 (9)
O ₂	0.3579 (2)	0.1120 (2)	0.5068 (1)	47 (2)	58 (2)	21.3 (6)	-8 (1)	-1.4 (7)	8.8 (8)
O ₃	0.2391 (2)	0.0118 (2)	0.3857 (1)	66 (2)	51 (2)	21.3 (6)	8 (1)	-7.9 (8)	-1.6 (8)
N ₁	0.0953 (2)	0.1619 (2)	0.5518 (1)	55 (2)	60 (2)	27.2 (9)	-15 (2)	9 (1)	-3 (1)
N ₂	0.4672 (2)	0.1461 (2)	0.5011 (1)	42 (2)	43 (2)	21.7 (7)	0 (1)	-3.4 (9)	2 (1)
N ₃	0.1970 (2)	0.0057 (2)	0.3174 (1)	54 (2)	54 (2)	20.4 (7)	4 (2)	-1.0 (9)	-4 (1)
C ₁₁	0.0294 (3)	0.0996 (3)	0.6020 (2)	117 (4)	90 (4)	41 (1)	-44 (3)	36 (2)	-6 (2)
C ₁₂	0.1224 (2)	0.2659 (3)	0.5564 (2)	50 (2)	60 (3)	25 (1)	-6 (2)	4 (1)	-3 (1)
C ₁₃	0.0915 (3)	0.3331 (3)	0.6180 (2)	79 (3)	73 (3)	29 (1)	-24 (2)	18 (1)	-8 (2)
C ₁₄	0.0150 (3)	0.4208 (3)	0.6075 (2)	96 (4)	76 (3)	50 (2)	-9 (3)	32 (2)	-11 (2)
C ₁₅	-0.0087 (5)	0.4870 (4)	0.6645 (4)	154 (6)	84 (4)	81 (3)	-22 (4)	72 (3)	-28 (3)
C ₁₆	0.0396 (7)	0.4687 (6)	0.7296 (4)	258 (10)	138 (7)	61 (3)	-60 (6)	82 (4)	-48 (4)
C ₁₇	0.1166 (6)	0.3819 (6)	0.7408 (3)	246 (9)	174 (7)	28 (2)	-61 (6)	32 (3)	-19 (3)
C ₁₈	0.1420 (4)	0.3126 (4)	0.6843 (2)	158 (5)	111 (4)	29 (1)	-17 (4)	18 (2)	-6 (2)
C ₂₁	0.5371 (3)	0.1264 (3)	0.5677 (2)	69 (3)	65 (3)	23 (1)	1 (2)	-11 (1)	6 (1)
C ₂₂	0.4983 (2)	0.1938 (2)	0.4435 (2)	47 (2)	36 (2)	22.7 (9)	2 (2)	1 (1)	1 (1)
C ₂₃	0.6201 (2)	0.2241 (2)	0.4349 (2)	49 (2)	46 (2)	27 (1)	-2 (2)	5 (1)	0 (1)
C ₂₄	0.6433 (3)	0.3271 (3)	0.4071 (2)	61 (3)	52 (3)	42 (1)	3 (2)	15 (1)	7 (2)
C ₂₅	0.7553 (3)	0.3588 (3)	0.3987 (2)	78 (3)	64 (3)	64 (2)	-10 (3)	26 (2)	12 (2)
C ₂₆	0.8437 (3)	0.2862 (4)	0.4158 (3)	53 (3)	92 (4)	69 (2)	-7 (3)	20 (2)	9 (2)
C ₂₇	0.8210 (3)	0.1830 (3)	0.4407 (2)	53 (3)	83 (4)	59 (2)	13 (2)	6 (2)	5 (2)
C ₂₈	0.7097 (3)	0.1508 (3)	0.4504 (2)	59 (3)	57 (3)	42 (1)	4 (2)	6 (1)	7 (2)
C ₃₁	0.2206 (3)	-0.1016 (3)	0.2855 (2)	101 (3)	57 (3)	29 (1)	20 (2)	-2 (2)	-12 (1)
C ₃₂	0.1388 (2)	0.0878 (3)	0.2876 (2)	45 (2)	58 (2)	23.1 (9)	2 (2)	0 (1)	-2 (1)
C ₃₃	0.0945 (3)	0.0834 (3)	0.2123 (2)	71 (3)	52 (2)	20.8 (9)	7 (2)	-2 (1)	-4 (1)
C ₃₄	-0.0209 (3)	0.1017 (3)	0.1958 (2)	76 (3)	81 (3)	26 (1)	-2 (2)	-10 (1)	-3 (1)
C ₃₅	-0.0629 (3)	0.1065 (3)	0.1253 (2)	110 (4)	70 (3)	36 (1)	-12 (3)	-29 (2)	4 (2)
C ₃₆	0.0097 (4)	0.0932 (3)	0.0720 (2)	154 (5)	61 (3)	23 (1)	1 (3)	-14 (2)	-1 (1)
C ₃₇	0.1231 (4)	0.0741 (4)	0.0875 (2)	162 (5)	89 (4)	23 (1)	29 (3)	15 (2)	-3 (2)
C ₃₈	0.1661 (3)	0.0706 (3)	0.1580 (2)	100 (3)	99 (4)	28 (1)	32 (3)	3 (2)	1 (2)

^a The form of the anisotropic thermal ellipsoid is $\exp[-(\beta_{11}h^2 + \beta_{22}k^2 + \beta_{33}l^2 + 2\beta_{12}hk + 2\beta_{13}hl + 2\beta_{23}kl)]$.

Table IV. Positional and Anisotropic Thermal Parameters ($\times 10^4$) for the Nonhydrogen Atoms of Fe(MTB)₃

atom	x	y	z	β_{11}^a	β_{22}	β_{33}	β_{12}	β_{13}	β_{23}
Fe	0.23549 (4)	0.15460 (4)	0.43564 (2)	42.3 (4)	48.5 (4)	17.0 (1)	-0.4 (3)	-0.9 (2)	-0.1 (2)
S ₁	0.18115 (7)	0.33013 (7)	0.49161 (4)	66.9 (7)	47.5 (7)	19.7 (3)	-5.0 (6)	3.3 (3)	-1.2 (3)
S ₂	0.39943 (7)	0.22562 (8)	0.37918 (4)	50.2 (7)	81.0 (8)	18.3 (3)	0.2 (6)	0.8 (3)	12.7 (4)
S ₃	0.11408 (7)	0.20895 (8)	0.33080 (4)	65.1 (8)	55.1 (7)	20.5 (3)	17.7 (6)	-8.2 (4)	-4.9 (4)
O ₁	0.1288 (2)	0.0961 (2)	0.5022 (1)	59 (2)	51 (2)	25.1 (8)	-10 (2)	10.4 (9)	-7 (1)
O ₂	0.3629 (2)	0.1139 (2)	0.5077 (1)	41 (2)	56 (2)	20.6 (7)	-6 (1)	-0.2 (8)	7.7 (9)
O ₃	0.2246 (2)	0.0093 (2)	0.3847 (1)	69 (2)	49 (2)	19.8 (7)	9 (2)	-8.2 (9)	-3.0 (9)
N ₁	0.1039 (2)	0.1581 (2)	0.5579 (1)	55 (2)	61 (2)	24.1 (9)	-8 (2)	9 (1)	-1 (1)
N ₂	0.4733 (2)	0.1456 (2)	0.5022 (1)	42 (2)	44 (2)	18.7 (8)	0 (2)	-3 (1)	4 (1)
N ₃	0.1860 (2)	0.0050 (2)	0.3162 (1)	53 (2)	56 (2)	18.6 (8)	3 (2)	-4 (1)	-4 (1)
C ₁₁	0.0482 (4)	0.0912 (4)	0.6100 (2)	132 (5)	93 (4)	33 (1)	-44 (4)	38 (2)	-3 (2)
C ₁₂	0.1229 (3)	0.2654 (3)	0.5595 (2)	48 (3)	57 (3)	23 (1)	-4 (2)	4 (1)	-4 (1)
C ₁₃	0.0966 (3)	0.3306 (3)	0.6227 (2)	84 (3)	63 (3)	30 (1)	-23 (3)	21 (2)	-10 (2)
C ₁₄	0.0197 (4)	0.4178 (4)	0.6152 (2)	95 (4)	79 (4)	50 (2)	-10 (3)	37 (2)	-16 (2)
C ₁₅	-0.0010 (5)	0.4827 (4)	0.6724 (4)	168 (7)	77 (4)	82 (3)	-21 (4)	78 (4)	-26 (3)
C ₁₆	0.0551 (8)	0.4611 (6)	0.7366 (4)	291 (12)	141 (8)	60 (3)	-81 (8)	94 (5)	-53 (4)
C ₁₇	0.1328 (7)	0.3758 (6)	0.7451 (3)	272 (10)	162 (7)	26 (2)	-71 (7)	34 (3)	-23 (3)
C ₁₈	0.1540 (4)	0.3097 (4)	0.6874 (2)	158 (6)	103 (4)	26 (1)	-18 (4)	16 (2)	-8 (2)
C ₂₁	0.5440 (3)	0.1250 (3)	0.5686 (2)	64 (3)	59 (3)	19 (1)	0 (2)	-11 (1)	6 (1)
C ₂₂	0.5030 (3)	0.1943 (3)	0.4452 (2)	51 (3)	35 (2)	20 (1)	1 (2)	0 (1)	3 (1)
C ₂₃	0.6246 (3)	0.2246 (3)	0.4370 (2)	47 (3)	46 (3)	22 (1)	-1 (2)	5 (1)	1 (1)
C ₂₄	0.6476 (3)	0.3279 (3)	0.4086 (2)	59 (3)	50 (3)	34 (1)	3 (2)	9 (2)	6 (2)
C ₂₅	0.7588 (3)	0.3603 (3)	0.4007 (2)	80 (4)	59 (3)	49 (2)	-12 (3)	19 (2)	9 (2)
C ₂₆	0.8488 (3)	0.2888 (4)	0.4193 (2)	49 (3)	82 (4)	50 (2)	-9 (3)	14 (2)	0 (2)
C ₂₇	0.8268 (3)	0.1851 (3)	0.4452 (2)	48 (3)	79 (4)	46 (2)	15 (3)	5 (2)	1 (2)
C ₂₈	0.7156 (3)	0.1520 (3)	0.4539 (2)	53 (3)	53 (3)	35 (1)	2 (2)	4 (1)	4 (2)
C ₃₁	0.2062 (3)	-0.1035 (3)	0.2846 (2)	115 (4)	61 (3)	27 (1)	24 (3)	-1 (2)	-12 (2)
C ₃₂	0.1357 (3)	0.0907 (3)	0.2848 (3)	43 (2)	55 (3)	20 (1)	3 (2)	-1 (1)	-4 (1)
C ₃₃	0.0938 (3)	0.0863 (3)	0.2091 (2)	79 (3)	49 (3)	19 (1)	6 (2)	0 (1)	-3 (1)
C ₃₄	-0.0213 (3)	0.1049 (3)	0.1898 (2)	77 (3)	74 (3)	25 (1)	-5 (3)	-9 (2)	2 (2)
C ₃₅	-0.0612 (4)	0.1096 (3)	0.1188 (2)	119 (5)	72 (4)	32 (1)	-15 (3)	-25 (2)	3 (2)
C ₃₆	0.0124 (5)	0.0946 (3)	0.0687 (2)	183 (6)	52 (3)	22 (1)	-7 (4)	-14 (2)	1 (2)
C ₃₇	0.1266 (5)	0.0761 (4)	0.0862 (2)	195 (7)	90 (4)	20 (1)	40 (4)	21 (2)	1 (2)
C ₃₈	0.1681 (4)	0.0725 (4)	0.1572 (2)	105 (4)	101 (4)	26 (1)	33 (3)	6 (2)	1 (2)

^a The form of the anisotropic thermal ellipsoid is $\exp[-(\beta_{11}h^2 + \beta_{22}k^2 + \beta_{33}l^2 + 2\beta_{12}hk + 2\beta_{13}hl + 2\beta_{23}kl)]$.

Table V. Positional and Anisotropic Thermal Parameters ($\times 10^4$) for the Nonhydrogen Atoms of Mn(MTB)₃

atom	<i>x</i>	<i>y</i>	<i>z</i>	β_{11}^a	β_{22}	β_{33}	β_{12}	β_{13}	β_{23}
Mn	0.23989 (3)	0.15546 (4)	0.43557 (2)	36.7 (3)	49.2 (4)	16.6 (1)	-1.4 (3)	-0.1 (1)	1.2 (2)
S ₁	0.18051 (7)	0.34057 (7)	0.49100 (4)	66.0 (7)	52.0 (6)	20.5 (2)	-6.8 (6)	4.8 (3)	0.2 (3)
S ₂	0.39686 (6)	0.21650 (7)	0.37785 (4)	44.3 (6)	75.1 (8)	17.8 (2)	-0.7 (5)	0.8 (3)	10.3 (3)
S ₃	0.11896 (7)	0.20081 (7)	0.33383 (4)	57.7 (6)	54.9 (7)	21.2 (2)	14.2 (5)	-6.4 (3)	-4.8 (3)
O ₁	0.1244 (2)	0.1030 (2)	0.4973 (1)	53 (2)	53 (2)	24.1 (7)	-13 (1)	10.9 (8)	-7.7 (9)
O ₂	0.3596 (2)	0.1160 (2)	0.5089 (1)	38 (1)	61 (2)	19.3 (6)	-7 (1)	0.3 (7)	8.3 (8)
O ₃	0.2280 (2)	-0.0023 (2)	0.3845 (1)	62 (2)	57 (2)	19.1 (6)	5 (1)	-7.8 (8)	-1.3 (9)
N ₁	0.1002 (2)	0.1650 (2)	0.5536 (1)	50 (2)	59 (2)	23.1 (8)	-10 (2)	9 (1)	-2 (1)
N ₂	0.4711 (2)	0.1473 (2)	0.5035 (1)	36 (2)	42 (2)	19.4 (7)	0 (2)	-2.3 (9)	3 (1)
N ₃	0.1887 (2)	-0.0036 (2)	0.3164 (1)	50 (2)	52 (2)	19.4 (7)	5 (2)	-1 (1)	-5 (1)
C ₁₁	0.0438 (3)	0.0975 (3)	0.6052 (2)	119 (4)	78 (4)	35 (1)	-43 (3)	34 (2)	-3 (2)
C ₁₂	0.1211 (2)	0.2721 (3)	0.5569 (2)	42 (2)	62 (3)	23 (1)	-2 (2)	4 (1)	-3 (1)
C ₁₃	0.0957 (3)	0.3349 (3)	0.6217 (2)	74 (3)	64 (3)	27 (1)	-19 (3)	18 (1)	-7 (2)
C ₁₄	0.0189 (3)	0.4229 (3)	0.6160 (2)	87 (3)	73 (4)	47 (2)	-10 (3)	31 (2)	-12 (2)
C ₁₅	0.0007 (4)	0.4854 (4)	0.6754 (3)	148 (6)	84 (4)	75 (2)	-15 (4)	72 (3)	-22 (3)
C ₁₆	0.0581 (7)	0.4609 (6)	0.7386 (3)	267 (10)	127 (6)	52 (2)	-57 (6)	84 (4)	-38 (3)
C ₁₇	0.1349 (6)	0.3743 (5)	0.7449 (2)	256 (9)	146 (6)	24 (1)	-53 (6)	31 (3)	-15 (2)
C ₁₈	0.1538 (4)	0.3103 (4)	0.6861 (2)	150 (5)	92 (4)	28 (1)	-10 (4)	17 (2)	-6 (2)
C ₂₁	0.5416 (3)	0.1278 (3)	0.5703 (2)	57 (3)	62 (3)	20.0 (9)	3 (2)	-10 (1)	7 (1)
C ₂₂	0.5014 (2)	0.1910 (2)	0.4452 (1)	43 (2)	36 (2)	20.7 (9)	-1 (2)	1 (1)	2 (1)
C ₂₃	0.6231 (2)	0.2223 (2)	0.4360 (2)	39 (2)	42 (2)	22.9 (9)	-1 (2)	4 (1)	0 (1)
C ₂₄	0.6441 (3)	0.3244 (3)	0.4068 (2)	48 (2)	53 (3)	37 (1)	3 (2)	12 (1)	7 (1)
C ₂₅	0.7565 (3)	0.3577 (3)	0.3979 (2)	68 (3)	62 (3)	53 (2)	-9 (2)	22 (2)	11 (2)
C ₂₆	0.8467 (3)	0.2870 (4)	0.4167 (2)	46 (3)	85 (4)	55 (2)	-9 (3)	17 (2)	0 (2)
C ₂₇	0.8266 (3)	0.1838 (3)	0.4436 (2)	44 (3)	84 (4)	46 (2)	8 (2)	2 (2)	3 (2)
C ₂₈	0.7152 (3)	0.1501 (3)	0.4529 (2)	48 (2)	52 (3)	34 (1)	2 (2)	2 (1)	5 (1)
C ₃₁	0.2065 (3)	-0.1112 (3)	0.2819 (2)	110 (4)	64 (3)	29 (1)	25 (3)	-3 (2)	-12 (2)
C ₃₂	0.1384 (2)	0.0828 (3)	0.2860 (2)	42 (2)	55 (3)	20.1 (9)	9 (2)	0 (1)	-4 (1)
C ₃₃	0.0953 (3)	0.0829 (3)	0.2104 (2)	69 (3)	51 (3)	19.9 (9)	7 (2)	-3 (1)	-3 (1)
C ₃₄	-0.0214 (3)	0.1014 (3)	0.1918 (2)	66 (3)	79 (3)	25 (1)	-5 (3)	-8 (1)	2 (2)
C ₃₅	-0.0624 (3)	0.1068 (3)	0.1215 (2)	98 (4)	71 (3)	33 (1)	-7 (3)	-25 (2)	4 (2)
C ₃₆	0.0110 (4)	0.0934 (3)	0.0700 (2)	161 (5)	50 (3)	21 (1)	-3 (3)	-14 (2)	0 (1)
C ₃₇	0.1262 (4)	0.0756 (4)	0.0868 (2)	164 (5)	91 (4)	20 (1)	30 (4)	17 (2)	0 (2)
C ₃₈	0.1684 (3)	0.0706 (3)	0.1575 (2)	94 (3)	104 (4)	26 (1)	30 (3)	7 (2)	1 (2)

^a The form of the anisotropic thermal ellipsoid is $\exp[-(\beta_{11}h^2 + \beta_{22}k^2 + \beta_{33}l^2 + 2\beta_{12}hk + 2\beta_{13}hl + 2\beta_{23}kl)]$.

Table VI. Bond Distances (Å) for M(MTB)₃

	M = Co	M = Cr	M = Fe	M = Mn
M-S ₁	2.2080 (9)	2.3843 (10)	2.4728 (10)	2.5838 (11)
M-S ₂	2.1989 (9)	2.3595 (11)	2.4280 (10)	2.3236 (10)
M-S ₃	2.2007 (9)	2.3586 (11)	2.4335 (10)	2.3536 (11)
mean ^a	2.203 (3)	2.367 (8)	2.445 (14)	2.420 (82)
M-O ₁	1.937 (2)	1.986 (2)	1.979 (2)	1.958 (2)
M-O ₂	1.926 (2)	1.965 (2)	1.994 (2)	1.941 (2)
M-O ₃	1.943 (2)	1.976 (2)	1.998 (2)	2.132 (2)
mean	1.935 (5)	1.976 (6)	1.990 (6)	2.011 (61)
mean S-C ₂	1.718 (2)	1.710 (3)	1.703 (3)	1.707 (6)
mean O-N	1.354 (3)	1.350 (3)	1.348 (4)	1.349 (8)
mean N-C ₁	1.467 (2)	1.468 (2)	1.468 (2)	1.471 (2)
mean N-C ₂	1.301 (2)	1.303 (3)	1.307 (2)	1.306 (4)
mean C ₂ -C ₃	1.479 (3)	1.484 (3)	1.485 (2)	1.487 (4)
mean phenyl C-C	1.379 (4)	1.377 (4)	1.378 (3)	1.378 (3)

^a The standard deviations in the means are computed from the larger of the variance, $\sigma^2(\bar{x}) = \Sigma(x - \bar{x})^2/[n(n-1)]$, or the average standard deviation, $1/\sigma^2(\bar{x}) = \Sigma(1/\sigma^2(x_i))$. Where means only are quoted, all observations (other than of phenyl C-C bonds) were within 2σ of the mean.

metal-ligand bonding geometry.

Leaving aside Mn(MTB)₃ for the moment (a special case because of the tetragonal Jahn-Teller distortion) and examining Co-, Cr-, and Fe(MTB)₃, we should first note that all three complexes have symmetrical d-electron distributions in the octahedral approximation (Co has the t_{2g}^6 , Cr the t_{2g}^3 , and Fe the $t_{2g}^3e_g^2$ configuration). Despite this, however, the trigonal twist angle decreases from 54.9° for Co through 48.7° for Cr to 42.9° for Fe; this angle is 60 and 0° for octahedral and trigonal-prismatic structures, respectively (see Figure 4). Concurrent with this decrease in twist angle, there is an increase in the mean M-S and M-O bond lengths (Table VI) and a decrease in the mean S-M-O angle (Table VII). As

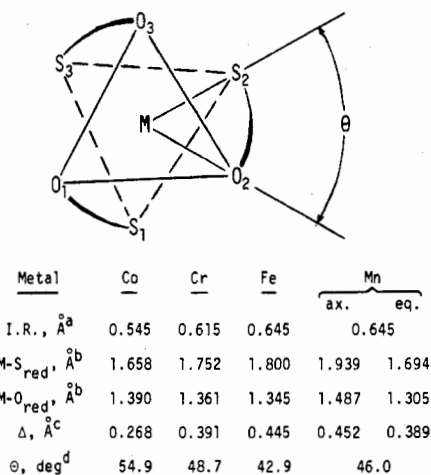


Figure 4. Comparison of the metal-ligand coordination geometries of the MTB complex. The tetragonal axis for the distortion Mn complex passes through atoms S₁ and O₃: (a) ref 16; (b) metal-ligand bond length minus the metal ionic radius; (c) difference between M-S and M-O bond lengths; (d) trigonal twist angle defined in the text and the above figure.

the thiohydroxamate chelate internal distances and angles change very little, except for the mean S-C₂ distance which decreases by 0.015 Å in going from Co(MTB)₃ to Fe(MTB)₃, the decrease in S-M-O angle and trigonal twist angle may, at least partially, be attributed to the increase in M-S and M-O bond lengths.

Two completely geometrical models which are similar in their predictions have been presented^{30,31} for the detailed analysis of tris(bidentate ligand) structures. In each the ligand bite, *b* (the ratio of the internal ligand chelate distance to the metal-ligand distance), and the trigonal twist angle, θ , are used

Table VII. Bond and Dihedral Angles (deg) for M(MTB)₃

	M = Co	M = Cr	M = Fe	M = Mn
S ₁ -M-O ₁	87.77 (7)	82.74 (7)	80.23 (7)	79.35 (7)
S ₂ -M-O ₂	87.00 (6)	82.44 (6)	79.72 (6)	82.78 (6)
S ₃ -M-O ₃	87.02 (6)	82.49 (6)	80.21 (6)	79.76 (6)
mean internal S-M-O ^a	87.3 (3)	82.6 (1)	80.0 (2)	80.6 (11)
S ₁ -M-O ₃	174.45 (7)	169.04 (6)	161.53 (7)	160.90 (6)
S ₂ -M-O ₁	173.16 (7)	169.77 (7)	166.09 (7)	171.14 (6)
S ₃ -M-O ₂	176.15 (7)	171.90 (6)	167.39 (7)	170.55 (6)
S ₁ -M-O ₂	92.13 (7)	94.08 (7)	96.77 (7)	96.80 (7)
S ₂ -M-O ₃	92.20 (7)	93.48 (7)	96.54 (7)	95.16 (6)
S ₃ -M-O ₁	95.34 (7)	99.10 (7)	105.38 (7)	100.11 (7)
S ₁ -M-S ₂	93.17 (3)	95.67 (4)	97.49 (4)	99.56 (4)
S ₁ -M-S ₃	91.45 (3)	91.32 (4)	88.28 (3)	88.46 (3)
S ₂ -M-S ₃	91.42 (4)	91.02 (4)	88.19 (4)	88.62 (4)
O ₁ -M-O ₂	86.19 (8)	87.58 (8)	86.90 (9)	88.61 (8)
O ₁ -M-O ₃	87.09 (9)	89.30 (9)	88.90 (9)	87.91 (8)
O ₂ -M-O ₃	89.54 (9)	93.09 (8)	97.50 (9)	97.07 (8)
mean M-S-C ₂	96.2 (3)	95.6 (6)	95.7 (10)	95.6 (22)
mean M-O-N	115.1 (3)	117.7 (7)	120.8 (8)	119.1 (10)
mean O-N-C ₁	111.7 (3)	111.6 (3)	111.5 (5)	111.5 (7)
mean O-N-C ₂	121.5 (3)	121.4 (3)	120.6 (3)	121.3 (5)
mean C ₁ -N-C ₂	126.7 (5)	127.0 (5)	127.5 (5)	127.1 (10)
mean S-C ₂ -N	118.9 (3)	119.8 (3)	120.2 (5)	120.3 (9)
mean S-C ₂ -C ₃	118.7 (1)	118.9 (2)	119.2 (3)	118.5 (4)
mean N-C ₂ -C ₃	122.3 (3)	121.3 (2)	120.7 (6)	121.2 (10)
dihedral angle I ^b				
1	6.0	13.4	18.3	22.2
2	8.5	6.6	4.3	6.0
3	11.3	13.7	14.6	15.9
dihedral angle II ^b				
1	73.8	67.1	61.8	62.3
2	43.8	45.0	43.4	45.8
3	56.7	56.8	60.0	60.8

^a The standard deviations in the means are computed from the variances, $\sigma^2(\bar{x}) = \Sigma(x - \bar{x})^2/[n(n-1)]$. ^b Dihedral angle I is the dihedral angle between the M-S-O plane and the S-C₂-N-O plane, for chelates 1-3. Dihedral angle II is the angle between the S-C₂-N-O plane and the phenyl plane, i.e., the torsion angle about the C₂-C₃ bond, for chelates 1-3.

in describing the variation from octahedral to trigonal-prismatic geometry. For catechol complexes an empirical relation between these two has been presented:²⁹ $\theta = (-73.9 + 94.10b)^\circ$. Although this ligand bite model cannot be used directly for these thiohydroxamate complexes because of the different M-S and M-O distances, the value of the twist angle may be seen to be dependent on the ligand bite, since this varies inversely with the M-L bond lengths. As was seen in the catecholate structures and is again seen here, a purely geometrical model fails to explain the large change in twist angle between the Fe and Cr structures accompanied by relatively small change in ligand bite. Wentworth³² has calculated the energy loss due to crystal field stabilization for various d-electron configurations as the octahedral geometry is systematically distorted toward trigonal prismatic. We ascribe a large part of the change in twist angle (from 55° for Co to 43° for Fe) to the ligand field effects of the d⁶, d³, and high-spin d⁵ electronic configurations, whose energy differences are in the range expected for the distortions observed.²⁹

A different approach of describing the variation from octahedral to trigonal-prismatic geometries is by using the dihedral angles between trigonal faces sharing common edges of the polyhedron.^{33,34} The ideal and observed dihedral angles for M(MTB)₃ complexes are given in Table IX, and these correspond to Figure 5. It is clear from the data presented that both the twist angle and dihedral angle treatments are in good agreement in the positions of the Co, Cr, and Fe complexes along the D_{3d}-D_{3h} reaction path, with the Co complex closest to the perfect octahedral geometry. The irregularity in the Cr complex is reflected by the ~5° difference between the dihedral angle at the S₃-O₁ edge and the

Table IX. Ideal and Observed Dihedral Angles (deg) for M(MTB)₃^a

complex	δ at b ₁	δ at b ₂	remaining δ
ideal octahedron	70.5, 70.5,	70.5, 70.5,	70.5, 70.5, 70.5
	70.5	70.5	70.5, 70.5, 70.5
ideal trigonal prism	0, 0, 0	120, 120,	90, 90, 90, 90,
		120	90, 90
Co(MTB) ₃	64.1, 66.3,	74.1, 74.5,	63.8, 66.3, 67.0,
	67.1	74.5	68.1, 73.8, 75.1
Cr(MTB) ₃	57.7, 62.8,	78.4, 79.6,	61.3, 63.3, 66.2,
	63.3	80.1	67.6, 72.6, 76.5
Fe(MTB) ₃	47.8, 59.6,	82.6, 83.0,	58.1, 59.6, 68.1,
	60.0	85.5	69.6, 72.2, 78.5
Mn(MTB) ₃	46.2, 64.4,	80.5, 82.5,	61.6, 62.7, 64.5,
	64.5	83.2	71.3, 72.8, 73.6

^a Cf. Figure 5 in this paper and ref 34.

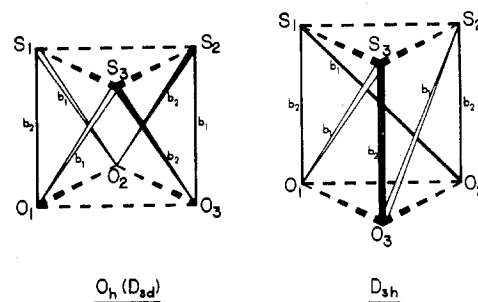


Figure 5. Six-atom family shape characteristics (see text).

other two b₁ edges. This difference is ~12° in the Fe complex—which shows a further distortion. In the Mn complex, which clearly shows a tetragonal distortion along the S₁-O₃ axis, the above difference is ~18°. In addition, the dihedral angles at the S₁-O₂ and S₂-O₃ edges are close to the corresponding dihedral angles in the Cr and Co complexes.

The virtual constancy of the S-C, C-N, and N-O bond lengths of the rings for each of the metal complexes shows that no substantial change in internal ligand bonding occurs in the series Co, Cr, Fe, and Mn. However, there is a dramatic shift in the difference of the M-S and M-O bond lengths, as noted in Figure 4. This difference is only 0.268 Å for Co, increases to 0.391 Å for Cr, and is 0.445 Å for Fe. Yet the M-O distances correspond well to ionic radius sums. Thus the anomaly is primarily in the very short Co-S bond length. All of the M-S bond lengths are essentially the same as those in other octahedral complexes containing sulfur ligating atoms.³⁵⁻⁴³ The only possible explanation for the unusually short M-S bond lengths for low-spin d⁶, low-spin d⁵, and (to a lesser extent) d³ metal ion complexes is metal-to-ligand back-bonding involving π* orbitals of the sulfur atoms. This results in a substantial increase of, for example, the Co-S bond order in the Co(MTB)₃ complex.

The Mn(MTB)₃ complex displays a substantial Jahn-Teller distortion due to the high-spin d⁴ state. Thus the mean M-S and M-O bond lengths are not useful for comparison due to the very large ranges (Table VI, Figure 4). If we calculate the tetragonal distortion as the ratio of the range of bond lengths to the mean bond length, Mn has a tetragonal distortion of 10.2% while Fe has 1.4%, Cr has 1.1%, and Co has only 0.7%. With the tetragonal distortion, the M-L distances can be divided into axial [M-S = 2.584 (1), M-O = 2.132 (2), Δ = 0.452 Å] and equatorial distances [M-S = 2.339 (15), M-O = 1.950 (9), Δ = 0.389 Å]. In the axial direction, where there is direct interaction of the ligand with the antibonding e_g electron of the Mn³⁺ ion just as there is in the Fe³⁺ complex, the differences in M-S and M-O bond lengths are nearly the same (0.452 and 0.445 Å for Mn and Fe, respectively). In contrast, in the equatorial directions the ligands see little interaction with the single (d_{x²-y²) e_g electron}

but instead a metal electronic configuration substantially the same as the d^3 Cr^{3+} ion, and the differences in M-S and M-O bond lengths are again similar (0.389 and 0.391 Å for Mn and Cr, respectively). In addition to this large tetragonal distortion, there is a smaller, but significant, distortion that increases in the series Co, Cr, and Fe. This can perhaps best be seen (Table VII) as an opening of the $\text{S}_1\text{-M-S}_2$ bond angles (from 93.2 to 99.6° for Co and Fe, respectively, vs. an average for the other two S-M-S angles of 91.4 and 88.5°) and the adjacent $\text{O}_2\text{-M-O}_3$ angles (which are 89.5 and 97.1° for Co and Fe, respectively, vs. an average for the other two O-M-O angles of 86.6 and 88.2°).

In summary, the structural systematics of the tris(thiohydroxamato)metal complexes reported here show (1) metal-oxygen bond lengths that correlate well with ionic radii changes, (2) pronounced decreases in M-S bond lengths due to back-bonding from t_{2g} filled metal orbitals to π^* sulfur orbitals, (3) an effect of the ligand field stabilization energy upon the trigonal twist angle of the complex, (4) a pronounced Jahn-Teller distortion in the Mn complex, which in the axial direction is similar to that for the d^5 Fe complex and in the equatorial is similar to that for the d^3 Cr complex, and (5) a general similarity of the structures which gradually change from the highly regular Co complex to the less regular Fe.

Acknowledgment. The microbial iron transport program is supported by the NIH (Grant RO1-AI11744). Structural studies are supported in part by the NSF (Grant CHE-7826574). We thank the U.S. AID for a fellowship to K.A.-D. and Dr. A. Cheetham for helpful discussions.

Registry No. $\text{Co}(\text{PhC}(=\text{S})\text{N}(\text{O})\text{CH}_3)_3$, 71341-73-6; $\text{Cr}(\text{PhC}(=\text{S})\text{N}(\text{O})\text{CH}_3)_3$, 71341-72-5; $\text{Fe}(\text{PhC}(=\text{S})\text{N}(\text{O})\text{CH}_3)_3$, 71341-71-4; $\text{Mn}(\text{PhC}(=\text{S})\text{N}(\text{O})\text{CH}_3)_3$, 71369-93-2.

Supplementary Material Available: Table VIII (least-squares planes through the thiohydroxamate chelate ring), Tables X-XIII (thermal parameters), Tables XIV-XVII (root-mean-square amplitudes of vibration), and Tables XVIII-XXI (structure factor amplitudes) (103 pages). Ordering information is given on any current masthead page.

References and Notes

- (1) Part 16: Harris, W. R.; Carrano, C. J.; Raymond, K. N. *J. Am. Chem. Soc.* **1979**, *101*, 2722-7.
- (2) U.S. AID Fellow.
- (3) Raymond, K. N. *Adv. Chem. Ser.* **1977**, No. 162, 33-54.
- (4) Neilands, J. B. "Microbial Iron Metabolism"; Academic Press: New York, 1974.
- (5) Smith, R. M.; Martell, A. E. "Critical Stability Constants"; Plenum Press: New York, 1976; Vol. IV, p 7.
- (6) Leong, J.; Raymond, K. N. *J. Am. Chem. Soc.* **1974**, *96*, 6628-30.
- (7) Leong, J.; Raymond, K. N. *J. Am. Chem. Soc.* **1975**, *97*, 293-6.
- (8) Isied, S. S.; Kuo, G.; Raymond, K. N. *J. Am. Chem. Soc.* **1976**, *98*, 1763-7.
- (9) Itoh, S.; Inuzuka, K.; Suzuki, T. *J. Antibiot.* **1970**, *23*, 542-5.
- (10) Egawa, Y.; Umino, K.; Ito, Y.; Okuda, T. *J. Antibiot.* **1971**, *24*, 124-30.
- (11) Abu-Dari, K.; Raymond, K. N. *Inorg. Chem.* **1977**, *16*, 807-12.
- (12) Mitchell, A. J.; Murray, K. S.; Newman, P. J.; Clark, P. E. *Aust. J. Chem.* **1977**, *30*, 2439.
- (13) Murray, K. S.; Newman, P. J.; Gatehouse, B. M.; Taylor, D. *Aust. J. Chem.* **1978**, *31*, 983-92.
- (14) Leong, J.; Bell, S. J. *Inorg. Chem.* **1978**, *17*, 1886-92.
- (15) Abu-Dari, K.; Cooper, S. R.; Raymond, K. N. *Inorg. Chem.* **1978**, *17*, 3394-7.
- (16) Shannon, R. D. *Acta Crystallogr., Sect. A* **1976**, *32*, 751-67.
- (17) Mizukami, S.; Nagata, K. *Chem. Pharm. Bull.* **1966**, *14*, 1249-55.
- (18) Collman, J. P.; Kittleman, E. T. *Inorg. Synth.* **1966**, *8*, 149-53.
- (19) Nagata, K.; Mizukami, S. *Chem. Pharm. Bull.* **1967**, *15*, 61-9.
- (20) Dietzel, R.; Thomas, Ph. Z. *Angew. Allg. Chem.* **1971**, *381*, 214-8.
- (21) Cambi, L.; Bacchetti, T.; Paglia, E. *Rend. Ist. Lomb. Acad. Sci. Lett. A* **1956**, *90*, 577-93.
- (22) The Enraf-Nonius Fortran IV system operates the CAD-4 diffractometer. In addition to locally written programs for the CDC 7600, the following programs of modifications were used: Zalkin's FORDAP Fourier program; Ibers' NUCLS, a group least-squares version of the Busing-Levy ORFLS program; ORFFE, a function and error program by Busing and Levy; ORTEP 2, by Johnson; RBANG, a program to handle rigid groups; MULTAN, a program series for direct-methods phase determination of Germain, Main, and Woolfson.
- (23) Abu-Dari, K.; Ekstrand, J. D.; Freyberg, D. P.; Raymond, K. N. *Inorg. Chem.* **1979**, *18*, 108-12.
- (24) Baker, E. C.; Brown, L. D.; Raymond, K. N. *Inorg. Chem.* **1975**, *14*, 1376-9.
- (25) Definitions of the indicators are $R = \sum \Delta / \sum |F_o|$ and $R_w = [\sum w \Delta^2 / \sum w |F_o|^2]^{1/2}$, and the error in an observation of unit weight is $[\sum w \Delta^2 / (N_o - N_v)]^{1/2}$, where $\Delta = |F_o - F_c|$, N_o is the number of observations, and N_v is the number of variables.
- (26) Cromer, D. T.; Mann, B. *Acta Crystallogr., Sect. A* **1968**, *24*, 321-4.
- (27) Stewart, R. F.; Davidson, E. T.; Simpson, W. T. *J. Chem. Phys.* **1965**, *42*, 3175-87. Cromer, D. T. *Acta Crystallogr.* **1963**, *18*, 17-23.
- (28) Supplementary material.
- (29) Raymond, K. N.; Isied, S. S.; Brown, L. D.; Fronczek, F. R.; Nibert, J. H. *J. Am. Chem. Soc.* **1976**, *98*, 1767-74.
- (30) Kepert, D. L. *Inorg. Chem.* **1972**, *11*, 1561-3.
- (31) Avdeef, A.; Fackler, J. P., Jr. *Inorg. Chem.* **1975**, *14*, 2002-6.
- (32) Wentworth, R. A. D. *Coord. Chem. Rev.* **1972-1973**, *9*, 171-87.
- (33) Porai-Koshits, M. A.; Aslanov, L. A. *Zh. Strukt. Khim.* **1972**, *13*, 266-76.
- (34) Muettterties, E. L.; Guggenberger, L. J. *J. Am. Chem. Soc.* **1974**, *96*, 1748-56.
- (35) The comparison structures are Co, Cr, Fe, and Mn morpholydicarbodithioates,^{36,37} Co, Cr, and Fe diethyldithiocarbamates,³⁸⁻⁴⁰ and Co, Cr, and Fe ethyl xanthates.⁴¹⁻⁴³
- (36) Healy, P. C.; Sinn, E. *Inorg. Chem.* **1975**, *14*, 109-15.
- (37) Butcher, R. J.; Sinn, E. *J. Chem. Soc., Dalton Trans.* **1975**, 2517-22.
- (38) Merlino, S. *Acta Crystallogr., Sect. B* **1968**, *24*, 1441-8.
- (39) Ralston, C. L.; White, A. M. *Aust. J. Chem.* **1977**, *30*, 2091-4.
- (40) Liepoldt, J. G.; Coppens, P. *Inorg. Chem.* **1973**, *12*, 2269-74.
- (41) Merlino, S. *Acta Crystallogr., Sect. B* **1969**, *25*, 2270-6.
- (42) Merlino, S.; Sartori, F. *Acta Crystallogr., Sect. B* **1972**, *28*, 972-6.
- (43) Hoskins, B. F.; Kelly, B. P. *J. Chem. Soc., Chem. Commun.* **1970**, 45-6.